Communication—Large Electron-Hole Diffusion Lengths in Methylammonium Lead Triiodide Perovskite Films Prepared by an Electrochemical-Chemical Approach

Lorena Macor,[a] Agustín Sigal,[b] Thomas Dittrich,[c] Jörg Rappich,[c] Luis Otero,[a] and Miguel Gervaldo[a,z]

[a]*Departamento de Química, Universidad Nacional de Río Cuarto, CONICET, Río Cuarto, 5800 Córdoba, Argentina*
[b]*Facultad de Matemática, Astronomía y Física, Universidad Nacional de Córdoba, Ciudad Universitaria, 5000 Córdoba, Argentina*
[c]*Helmholtz-Zentrum Berlin für Materialien und Energie GmbH, Institut für Silizium-Photovoltaik, 12489 Berlin, Germany*

Methylammonium lead triiodide ($CH_3NH_3PbI_3$) perovskite films were generated by chemical conversion of PbO_2 layers electrodeposited over NiO hole selective contact, by simple immersion in CH_3NH_3I isopropanol solution under ambient conditions. 2.4 μm charge carrier diffusion lengths were measured by surface photovoltage, being these very similar to the size of the as formed perovskite crystals, showing that there are not deleterious encounters with defects or impurities. The electrochemical procedure used here demonstrates the capacity of this technique for the fabrication of perovskite films with large electron-hole diffusion lengths by solution based processes using only water and isopropanol.
© 2017 The Electrochemical Society. [DOI: 10.1149/2.0181712jss] All rights reserved.

Currently, great efforts are focused on the development of new fabrication processes that allow large scale production and long-term stability to organometallic halide perovskite based solar cells, in order to make their manufacturing and commercialization possible.[1–4] It has been shown that large grains (up to 10 μm) having low bulk defects present large electron and hole diffusion lengths,[5] permitting the photogenerated charge carriers the propagation through the device, without deleterious encounters with defects or impurities.[6] Moreover, increases in power conversion efficiencies of perovskite solar cells have been obtained in correlation with the increase in the charge-carrier transport lengths. In the same way, a linear increase between the grain size and the electron-hole diffusion length has been demonstrated.[7] Also, it has been shown that the chemical conversion of electro-deposited lead dioxide (PbO_2) films by immersion in methylammonium iodide (MAI) produces perovskite films with low trap densities and higher photoluminescence than films produced by spin coating.[8] However, there are other deposition methods that can produce perovskite films with improved optoelectronic properties.[9] In these materials the diffusion lengths of photo-generated charge carriers in $CH_3NH_3PbI_3$ perovskites can be directly measured by modulated Surface Photovoltage (SPV) with high accuracy.[5,7] The methodology developed by Goodman[10] allows quick and reliable evaluation of electron-hole diffusion lengths in photoelectrodes.[5,7,10]

In this communication, we report the formation of $CH_3NH_3PbI_3$ perovskite films generated by one step chemical conversion of PbO_2 layers, by immersion in isopropanol MAI solution under ambient conditions. Both, NiO (hole selective contact) and PbO_2 were deposited by a simple electrochemical methodology in water solutions. Electron-hole diffusion lengths of 2.4 μm were obtained in the as formed perovskite films by SPV measurements. For comparison purposes, $CH_3NH_3PbI_3$ was also formed from PbI_2 films prepared by the usual spin coating procedure on NiO layer. The electrochemical methodology here reported could be very important in the fabrication of highly homogeneous large area solar cells at industrial scale production involving only solution based procedures in water and isopropanol.

Experimental

$CH_3NH_3PbI_3$ perovskite films were prepared as follows. First $Ni(OH)_2$ was electrodeposited on FTO substrates (area: 1 cm^2) at -0.25 mA/cm^2 for 2 min using a 0.02 M nickel nitrate solution in deionized water. The $Ni(OH)_2$ film was annealed at 350°C for 30 min

to form NiO, with a thickness of about 100 nm.[11] A PbO_2 layer was electrodeposited over the NiO layer at a fixed potential of +0.30 Volt vs Ag/AgCl for 2 min at 50°C (0.1 M $Pb(NO_3)_2$ and 5 M NaOH in deionized water). For comparison purposes, PbI_2 was spin coated over the FTO/NiO substrates at 3000 rpm (N_2-filled glove box), employing a 1 M PbI_2 solution in DMF. The perovskite films were generated by chemical conversion of PbO_2 and PbI_2 films by immersion in 0.1 M MAI solution in isopropanol (60 minutes for FTO/NiO/PbO_2 and 60 seconds for FTO/NiO/PbI_2) under ambient conditions to ensure complete conversion in perovskite. Then, the different chemically converted films were annealed at 100° for 30 min.

The morphologies, crystal sizes, coverage, and thicknesses of the films were studied by Scanning Electron Microscopy (SEM, Sigma Zeiss, working at 5 kV). Film thicknesses and uniformities were also analyzed by profilometry (Bruker Dektak 8 step-profiler). X-ray diffraction was used to confirm the chemical conversion of PbO_2 and PbI_2 films into $CH_3NH_3PbI_3$ (Philips PW1800/10, with a Cu-Kα radiation source). Modulated SPV measurements[5,7] were carried out to investigate both separation direction and diffusion lengths of the photo generated charge carriers of the $CH_3NH_3PbI_3$ perovskite films. In the construction of Goodman plots the absorption length of the $CH_3NH_3PbI_3$ perovskite was taken from literature.[5,7]

Results and Discussion

Top view SEM images of FTO, FTO/NiO, FTO/NiO/PbO_2, FTO/NiO/PbI_2, and films of perovskite obtained from FTO/NiO/PbO_2 and from FTO/NiO/PbI_2 are shown in Fig. 1. FTO substrate presents grains distributed unevenly with irregular shapes and obvious grain boundaries, while NiO exhibits a flowerlike structure (Figs. 1a–1b).[12] PbO_2 surface seems to be formed by aggregates of needles (Fig. 1c). Contrarily, PbI_2 spin coated on NiO features an uneven and inhomogeneous surface (Fig. 1d). When PbO_2 film is chemically converted in perovskite, the crystals are distributed homogeneously, and present a rectangular shape with sizes ranging from 600 nm to about 2 μm (Fig. 1e). On the other side, as shown in Fig. 1f and inset Fig. 1f, the chemical conversion of PbI_2 produces a large amount of perovskite crystals with sizes of around 50–100 nm. Only a few crystals with dimension of 400–600 nm are observed.

Fig. 2 shows XRD patterns obtained after chemical conversion of FTO/NiO/ PbO_2 and FTO/NiO/PbI_2 films, and the XRD signals of FTO/NiO/ PbO_2 layer. PbO_2 layer presents peaks at 32.6°, 36.5°, and 49.6° assigned to the (101), (200), and (210) planes of tetragonal β-PbO_2, and one more peak at 28.8° assigned to the (111) plane of α-PbO_2 (Fig. 2a, red hash marks).[4,8,13] The NiO related peak (observed
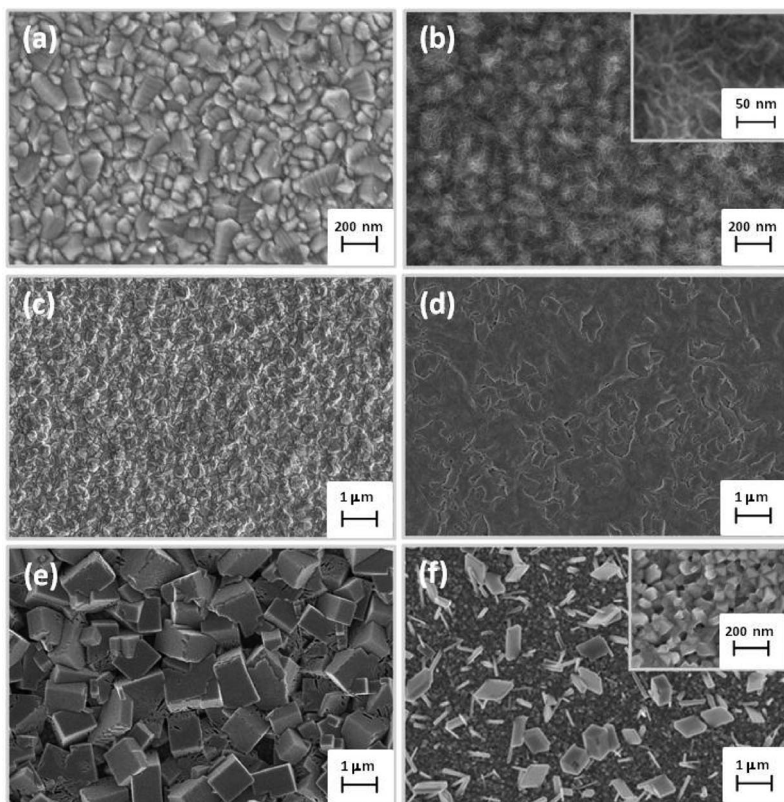
[z]E-mail: mgervaldo@exa.unrc.edu.ar

Figure 1. Top view SEM images of FTO (a), FTO/NiO (b), FTO/NiO/PbO$_2$ (c), FTO/NiO/PbI$_2$ (d), FTO/NiO/CH$_3$NH$_3$PbI$_3$ obtained by chemical conversion of FTO/NiO/PbO$_2$ (e), and by chemical conversion of FTO/NiO/PbI$_2$ (f).

at 37.25° for (111))[14,15] is probably superimposed with the FTO signal (Fig. 2a, black asterisks). After chemical conversion of PbO$_2$ (Fig. 2b), peaks at 14.2° (110), 24.7° (202), 28.4° (220), 31.9° (310), 39.6° (214),[16] 40.6° (224), and 43.2° (314) appear, and all peaks related to PbO$_2$ disappear, confirming the conversion of PbO$_2$ by CH$_3$NH$_3$I into CH$_3$NH$_3$PbI$_3$.[17,18] On the other hand, after chemical conversion of PbI$_2$ (Fig. 2c), the XRD pattern mainly presents the same diffraction peaks than those observed after chemical conversion of PbO$_2$. However, the relation between the intensity of the peaks associated to the FTO to the ones related to the perovskite differs between Figure b and c. This could be due to a difference in the amount of perovskite crystals obtained by the two different synthetic methodologies, in relation with the FTO.

Figs. 3a and 3b show the in-phase and phase-shifted by 90° modulated SPV spectra of the CH$_3$NH$_3$PbI$_3$ perovskite films obtained by chemical conversion of PbO$_2$ and PbI$_2$. In both cases the in-phase signal is negative, indicating that the electrons are preferentially separated toward the external surface,[5,19] while the holes are separated in the direction of the p-type NiO layer. The direction of this charge separation is in agreement with the fact that NiO is a p-type semiconductor, commonly used as hole transport layer in inverted perovskite solar cells.[11] The in-phase and phase shifted by 90° signals for both perovskite films present opposite signs, which indicates that the charge separation is produced by only one mechanism (Figs. 3a–3b). Both SPV spectra present an on-set signal at around 1.5 eV, which corresponds to the bandgap of both perovskite films, in good agreement with values reported for CH$_3$NH$_3$PbI$_3$.[18,20]

Goodman plots[5,7,10] were used to obtain averaged diffusion length values (L), in perovskite films, obtained by chemical conversion of PbO$_2$ and PbI$_2$. For perovskite films generated from PbI$_2$, diffusion lengths of (0.4 ± 0.1) μm are obtained (Fig. 4a), while perovskite formed from PbO$_2$ films, diffusion lengths as long as (2.4 ± 0.1) μm are observed (Fig. 4b). The large diffusion length value determined for the perovskite films generated from PbO$_2$ films is very similar to the size of the grains that dominate the perovskite covered surface area, indicating that this size probably limits the diffusion length of the perovskite films.[5,7]

Summary

CH$_3$NH$_3$PbI$_3$ perovskite films were successfully formed by chemical conversion of PbO$_2$ layers electro-deposited over NiO, by simple immersion in a CH$_3$NH$_3$I isopropanol solution under ambient conditions. The NiO bottom layer, used as hole selective contact, was also electrochemically grown in aqueous solution. The diffusion lengths in perovskite photoelectrodes obtained by chemical conversion of PbO$_2$ films were nearly one order of magnitude larger than those measured
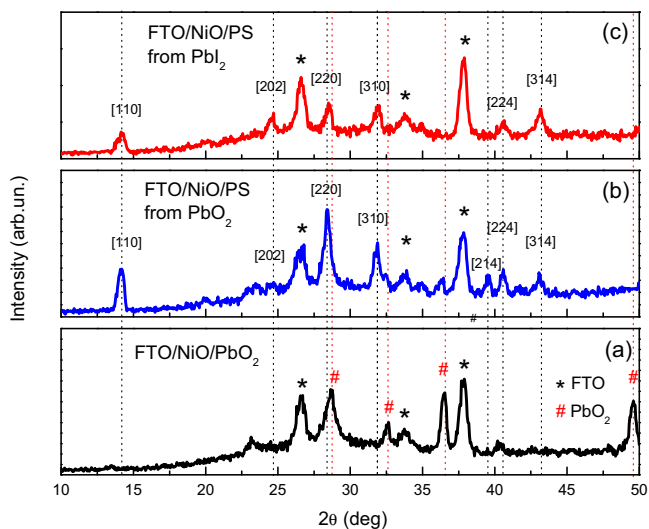

Figure 2. XRD patterns of FTO/NiO/PbO$_2$ before chemical conversion (a), CH$_3$NH$_3$PbI$_3$ obtained by chemical conversion of FTO/NiO/PbO$_2$ (b), and by chemical conversion of FTO/NiO/PbI$_2$ (c).

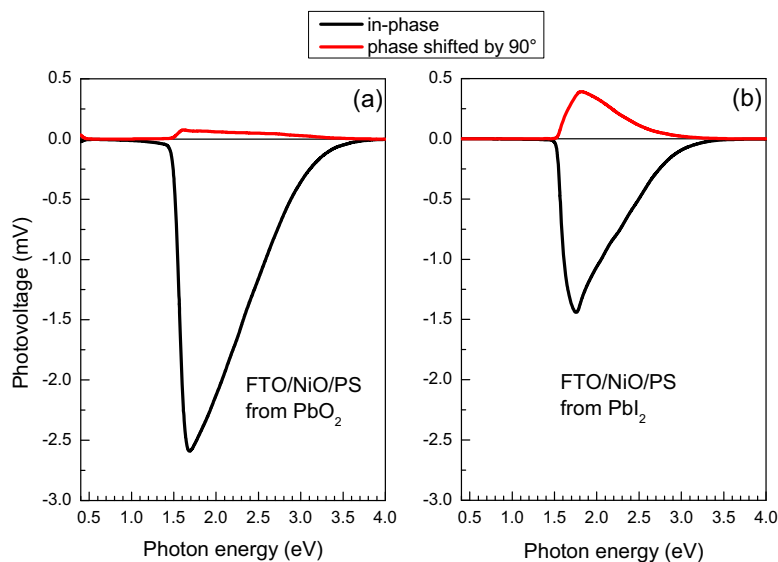**Figure 3.** Modulated in-phase (black lines) and phase-shifted by 90 (red lines) SPV spectra of $CH_3NH_3PbI_3$ layers obtained from chemical conversion of $FTO/NiO/PbO_2$ (a) and $FTO/NiO/PbI_2$ (b).

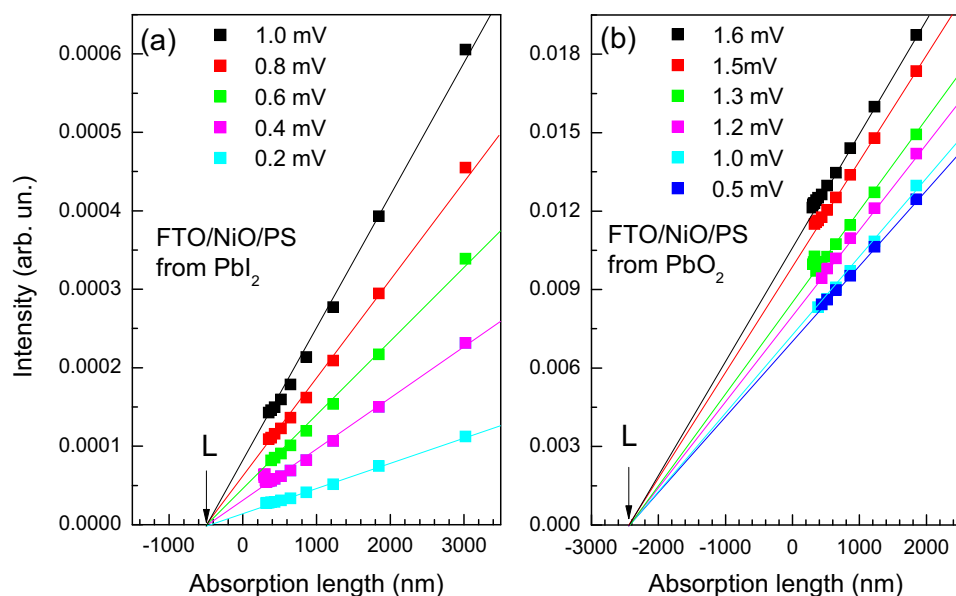**Figure 4.** Goodman plots measured for different constant SPV signals of $CH_3NH_3PbI_3$ obtained from chemical conversion of $FTO/NiO/PbI_2$ (a) and $FTO/NiO/PbO_2$ (b).

in photoelectrodes produced by the standard two step spin coating methodology. 2.4 μm charge carrier diffusion lengths were measured by surface photovoltage, being these very similar to the size of the as formed perovskite crystals. Finally, the presented electrochemical-chemical preparation route is a very promising methodology for the manufacturing of very uniform $CH_3NH_3PbI_3$ perovskite films and for the use of these layers in the fabrication of efficient perovskite based solar cells.

References

1. C. A. Ubani, M. A. Ibrahim, and M. A. M. Teridi, *Renew. Sust. Energ. Rev.*, **72**, 907 (2017).
2. S. Razza, S. Castro-Hermosa, A. Di Carlo, and T. M. Brown, *APL Mater.*, **4**, 091508 (2016).
3. J. Zhang, X. Gao, Y. Deng, B. Li, and C. Yuan, *ChemSusChem*, **8**, 3282 (2015).
4. H. Chen, Z. Wei, X. Zheng, and S. Yang, *Nano Energy*, **15**, 216 (2015).
5. Th. Dittrich, F. Lang, O. Shargaieva, J. Rappich, N. H. Nickel, E. Unger, and B. Rech, *Appl. Phys. Lett.*, **109**, 073901 (2016).
6. W. Nie, H. Tsai, R. Asadpour, J-C. Blancon, A. J. Neukirch, G. Gupta, J. J. Crochet, M. Chhowalla, S. Tretiak, M. A. Alam, H.-L. Wang, and A. D. Mohite, *Science*, **347**(6221) 522 (2015).
7. O. Shargaieva, F. Lang, J. Rappich, Th. Dittrich, M. Klaus, M. Meixner, C. Genzel, and N. H. Nickel, *Appl. Mater. Interfaces*.
8. J. A. Koza, J. C. Hill, A. C. Demster, and J. A. Switzer, *Chem. Mater.*, **28**, 399 (2016).
9. L. Qiu, L. K. Ono, and Y. Qi, *Mater. Today Energy*.
10. A. M. Goodman, *J. Appl. Phys.*, **32**, (12) 2550 (1961).
11. A. Subbiah, A. Halder, S. Ghosh, N. Mahuli, G. Hodes, and S. K. Sarkar, *J. Phys. Chem. Lett.*, **5**, 1748 (2014).
12. Z. H. Ibupoto, K. Khun, V. Beni, and M. Willander, *Soft Nanosci. Lett.*, **3**, 46 (2013).
13. Y. Tang and C. Kong, *Mater. Chem. Phys.*, **135**, 1108 (2012).
14. N. Dharmaraj, P. Prabu, S. Nagarajan, C. H. Kim, J. H. Park, and H. Y. Kim, *Mater. Sci. Eng. B*, **128**, 114 (2006).
15. H. Yan, D. Zhang, J. Xu, Y. Lu, Y. Liu, K. Qiu, Y. Zhang, and Y. Luo, *Nano Res. Lett.*, **9**, 424 (2014).
16. G. R. Kumar, A. D. Savariraj, S. N. Karthick, S. Selvam, B. Balamuralitharan, H.-J. Kim, K. K. Viswanathan, M. Vijaykumar, and K. Prabakar, *Phys. Chem. Chem. Phys.*, **18**, 7284 (2016).
17. G. Murugadoss, H. Kanda, S. Tanaka, H. Nishino, S. Ito, H. Imahoric, and T. Umeyama, *J. Power Sources*, **307**, 891 (2016).
18. T. Baikie, Y. Fang, J. M. Kadro, M. Schreyer, F. Wei, S. G. Mhaisalkar, M. Gratzel, and T. J. White, *J. Mater. Chem. A*, **1**, 5628 (2013).
19. L. Barnea-Nehoshtan, S. Kirmayer, E. Edri, G. Hodes, and D. Cahen, *J. Phys. Chem. Lett.*, **5**, 2408 (2014).
20. H-S Kim, C-R Lee, J-H Im, K-B Lee, T. Moehl, A. Marchioro, S.-J. Moon, R. Humphry-Baker, J.-H. Yum, J. E. Moser, M. Gratzel, and N. G. Park, *Sci. Rep.*, **2**, 591 (2012).